Microchimica Acta (2020) 187:408
https://doi.org/10.1007/s00604-020-04383-8

SHORT COMMUNICATION

PEG-PtS_2 nanosheet-based fluorescence biosensor for label-free human papillomavirus genotyping

Wenxian Zhang[1] · Shenchang Li[1] · Xiuping Li[1] · Man Liu[1] · Tianyu Cui[1] · Huayang Fu[2] · Mengsu Yang[2] · Wenying Zhong[1] · Bo Xu[1] · Wanqing Yue[1,3]

Received: 24 February 2020 / Accepted: 10 June 2020

Abstract

A simple and efficient ultrasonication-assisted liquid exfoliation method is proposed to produce PtS_2 nanosheets on a large scale and improve their dispersion in aqueous solution by surface polyethylene glycol modification. The interaction of polyethylene glycol-modified PtS_2 (PEG-PtS_2) nanosheets with fluorescent labeled DNA and the fluorescence quenching mechanism using FAM-labeled hpv16e6 gene fragment as a probe was investigated. The excitation and emission wavelengths were 468 and 517 nm, respectively. The fluorescence quenching mechanism of PEG-PtS_2 nanosheets for double-stranded DNA (dsDNA) might stem from the static quenching effect. Based on the difference in fluorescence quenching capability of PEG-PtS_2 nanosheets in fluorescent probe tagged single-stranded DNA (ssDNA) and dsDNA, a mix-and-detect method was proposed for determination of DNA. Without the need for probe immobilization and tedious washing steps, the genotyping of human papillomavirus (HPV) was easily achieved. The limit of detection was calculated to 0.44 nM, showing a good linear range within 0.05–10 nM. We believe this biosensor provides opportunities to develop a simple and low-cost strategy for molecular diagnostics.

Keywords Platinum disulfide nanosheets · DNA fluorescence biosensor · Ultrasonication-assisted liquid exfoliation method · Polyethylene glycol modification

Introduction

To perform high-sensitive and low-cost nucleic acid analysis, great progress has been made in the development of signal amplification and detection methods [1], in which nanomaterials have been widely used in ultra-sensitive DNA detection [2, 3]. Human papillomavirus (HPV) infection and sustained expression have an important causal relationship with cervical cancer, so HPV can be used as a biomarker for early screening of cervical cancer [4]. Currently, at least 100 types of HPV have been identified. Even though most HPV infections clear spontaneously and appear uninjurious to humans, continued infection with high-risk HPV (especially type 16) can lead to anal cancer, cervical cancer, vaginal cancer, and so on [4, 5]. Because HPV cannot be effectively cultured and serological tests have poor clinical performance, the diagnosis of HPV infection is almost completely dependent on molecular tools [6]. Therefore, it would be beneficial to develop an HPV genotyping method with high sensitivity and simplicity [1]. Recently, fluorescent DNA assay has aroused great interest and been widely exploited for various researches and applications [7].

Wenxian Zhang and Shenchang Li contributed equally to this work.

Electronic supplementary material The online version of this article (https://doi.org/10.1007/s00604-020-04383-8) contains supplementary material, which is available to authorized users.

✉ Bo Xu
xubo@cpu.edu.cn

✉ Wanqing Yue
yuewq@cpu.edu.cn

[1] School of Science, Key Laboratory of Biomedical Functional Materials, China Pharmaceutical University, Nanjing, People's Republic of China

[2] Department of Biomedical Sciences, City University of Hong Kong, 83 Tat Chee Avenue, Kowloon, Hong Kong SAR, People's Republic of China

[3] Key Laboratory of Drug Quality Control and Pharmacovigilance (China Pharmaceutical University), Ministry of Education, Nanjing, People's Republic of China

Published online: 29 June 2020

Two-dimensional (2D) transition metal dichalcogenides (TMDCs) are the most promising nanomaterials for the advancement of electronics in the future. In recent years, for example, MoS_2 [8, 9], WS_2 [8, 10], and TaS_2 [10], have received increasing research interests [11]. Compared with bulk counterparts, these TMDC sheets have the characteristics of 2D morphology and ultra-thin thickness, and they have many unusual physical, chemical, and electronic properties, so they have multifarious applications [11]. These 2D nanostructures, due to their chemical and electronic activity, show great potential in the fields of opto-electronic/electronics [11, 12], electrocatalysis [13], sensors [14, 15], and energy storage [16]. The 10-group metal-based TMDCs, which have the advantages of large adjustable band gap, high air stability, and good electrical conductivity, have attracted great interest recently [17]. A representative example of this family is PtS_2, which can be synthesized in one step by directly selenizing (or sulfuring) the Pt thin film [17]. Using low-cost ultrasound liquid exfoliation method, Tsang et al. had produced PtS_2 microflakes and PtS_2 nanosheets successively [18, 19]. Similar to most metal sulfide compounds, PtS_2 nanosheets can be modified on the lamellar structure surface through non-covalent action, which can improve the dispersibility of 2D nanosheet materials [20]. As far as we know, there is no report of using PtS_2 or surface-modified PtS_2 nanosheets as sensing biosensors.

Herein, for the first time, we reported a simple and homogeneous assay format for DNA determination by using the PEG-PtS_2 nanosheet-based fluorogenic nanoprobes. PtS_2 is a kind of TMDCs, and the weak van der Waals force makes it easier to be exfoliated into nanosheets by an ultrasonication-assisted liquid exfoliation (USLE) method. The as-fabricated PtS_2 nanosheets were further modified by polyethylene glycol (PEG) to improve its dispersity in water. Without the need for immobilization of DNA fluorescent probe and tedious washing process, the dsDNA after hybridization could be directly distinguished in the presence of PtS_2 nanosheets. The sensitivity and selectivity of DNA fluorescence biosensor were evaluated and successfully demonstrated for the determination of HPV16 genotype.

Result and discussion

The proposed mix-and-detect strategy is schematically depicted in Scheme 1. PtS_2 was exfoliated into nanosheets

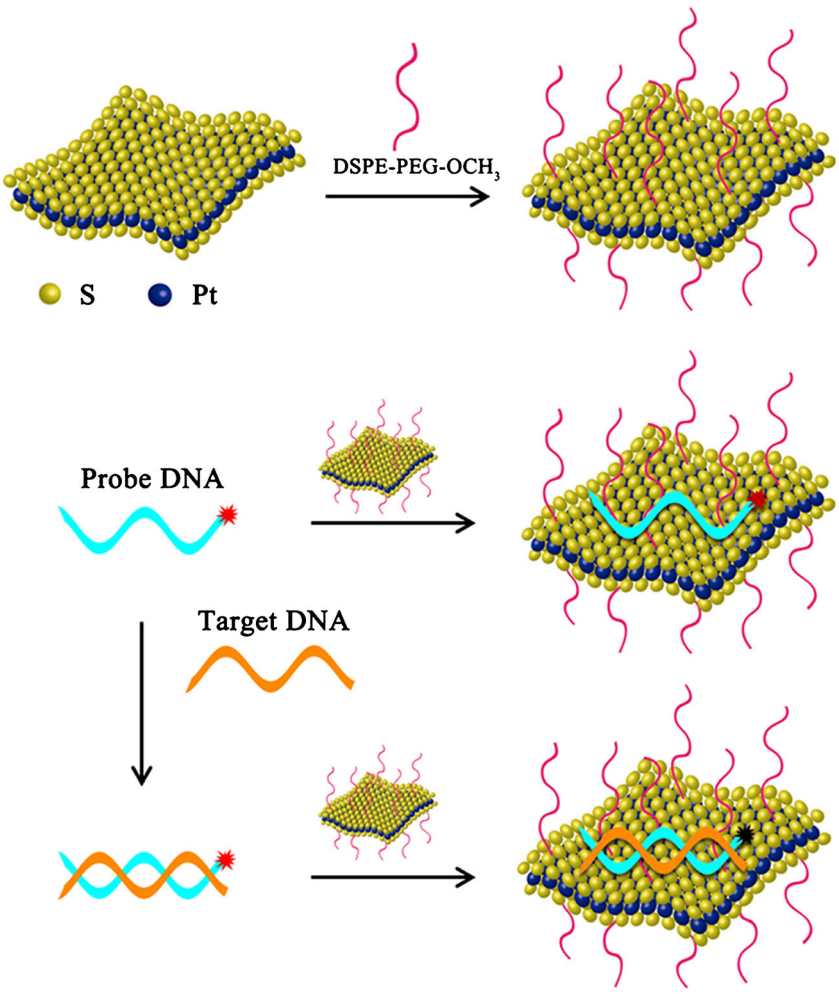

Scheme 1 Schematic illustration of PEG-PtS_2 nanosheet-based fluorescence biosensor for human papillomavirus genotyping

by an USLE method and further modified by PEG to improve its dispersity in water. In presence of PEG-PtS_2 nanosheets, the fluorescent intensity of tagged double-stranded DNA (dsDNA) after hybridization was dramatically decreased due to fluorescence quenching. Therefore, a fluorescence biosensor for DNA determination was constructed.

In our experiments, PtS_2 nanosheets were synthesized from the layered bulk PtS_2 by an USLE method. As-made PtS_2 nanosheets, although well dispersed in water, would precipitate and accumulate within 20 min. In order to improve the solubility of PtS_2 nanosheet, a distearoyl phosphoethanolamine-PEG2000 (DSPE-PEG-OCH_3) was thus synthesized and used to modify the surface of PtS_2 nanosheets through the Pt-S bond.

The as-fabricated PEG-PtS_2 nanosheets displayed a plate-shaped nanostructures (Fig. 1a, b). As shown in the image snapped by area electron diffraction under the high-resolution transmission electron microscopy (Fig. 1c), the material exhibited a sixfold symmetry, indicating the hexagonal single crystallinity. The X-ray photoelectron spectroscopy (XPS) Pt 4f core-level spectrum (Fig. 1d) revealed two peaks at 75.6 eV and 72.3 eV, which attributed to the doublet Pt 4f 5/2 and Pt 4f 7/2, respectively. The peaks of 164.2 eV and 162.3 eV in the XPS S 2p core-level spectrum (Fig. 1e) correspond to the S 2p 1/2 and S 2p 3/2 orbits of divalent sulfide ions (S^{2-}). The peak at 168.9 eV was corresponding to the SO_4^{2-}.

In order to evaluate the fluorescence quenching ability of PEG-PtS_2 nanosheets to the dye-labeled ssDNA/dsDNA, the fluorescent spectra upon evenly mixing the fluorescent probe and the synthesized PEG-PtS_2 nanosheets in the liquid phase were recorded. In this study, we used HPV16 genotype as target DNA, and designed sequences of FAM-labeled ssDNA probe (P) as well as the target DNA (T), respectively (Table S1). As shown in Fig. 2a, in the absence of PEG-PtS_2 nanosheets, strong fluorescence emission (black curve) was observed for the ssDNA probe (P), and the fluorescence intensity was decreased (red curve) after the addition of PEG-PtS_2 nanosheets. With the formation of dsDNA (P/T duplex) by hybridization of an equal amount of probe (P) with target DNA (T), the quenching fluorescence of probe (P) was further decreased in the presence of PEG-PtS_2 (green curve in Fig. 2a). These results indicated that PEG-PtS_2 nanosheets can quench the fluorescence of ssDNA and dsDNA.

Based on the aforementioned results, we deduced that the PEG-PtS_2 nanosheets have the potential as novel materials for DNA quantitative fluorescence determination. Subsequently,

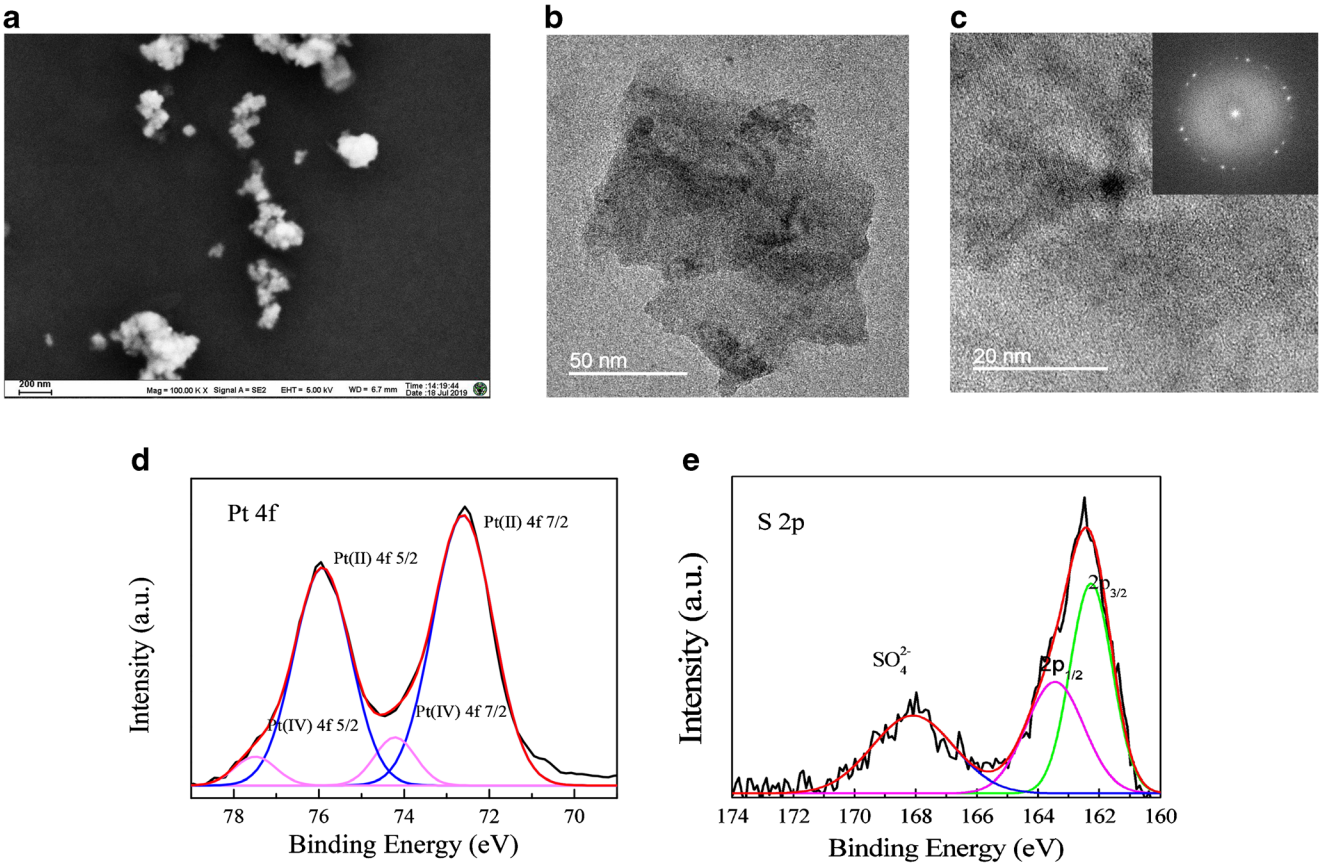

Fig. 1 Characterization of PEG-PtS_2 nanosheets. **a** SEM image, **b**, **c** TEM images (the inset is the corresponding selected area electron diffraction pattern), and **d**, **e** XPS spectra of PEG-PtS_2 nanosheets

HPV16 target DNA (0–50 nM) and FAM-tagged probe DNA (10 nM) of different concentrations were hybridized at a temperature of 50 °C, followed by the addition of PEG-PtS_2 nanosheets with a final concentration of 15.0 μg mL^{-1}. After incubation for 10 min, fluorescence measurement was performed (Fig. 2b, c). Therefore, the concentration of the target DNA could be quantified by the quenching of the fluorescence in the mixture of PtS_2 nanosheets. The determination process was very facile without the need of immobilization of probe DNA and tedious washing steps. We further evaluated the dynamic range and limit of detection (LOD) of the novel DNA fluorescent biosensor. A good linear relationship was established in the concentration range between 0.05 and 10 nM, and LOD was calculated as 0.44 nM (inset in Fig. 2d). Compared with recently reported optical methods based on nanomaterial for HPV determination (Table S2 of ESM), the LOD in this work was relatively low, but the detection range was relatively narrow, which was related to the limitation of determination methods. Meanwhile, the response time of this work was much shorter than that of other reported methods with comparable LOD. This mix-and-detect assay was designed for homogeneous determination of DNA

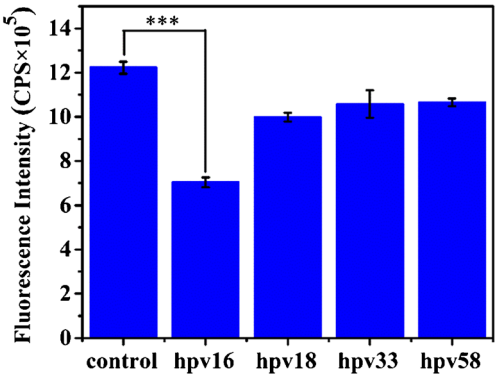

Fig. 3 Selectivity of the PEG-PtS_2 nanosheet-based biosensor in presence of different HPV types. The excitation and emission wavelengths are 468 and 517 nm, respectively. The error bars represented standard deviation of four parallel experiments

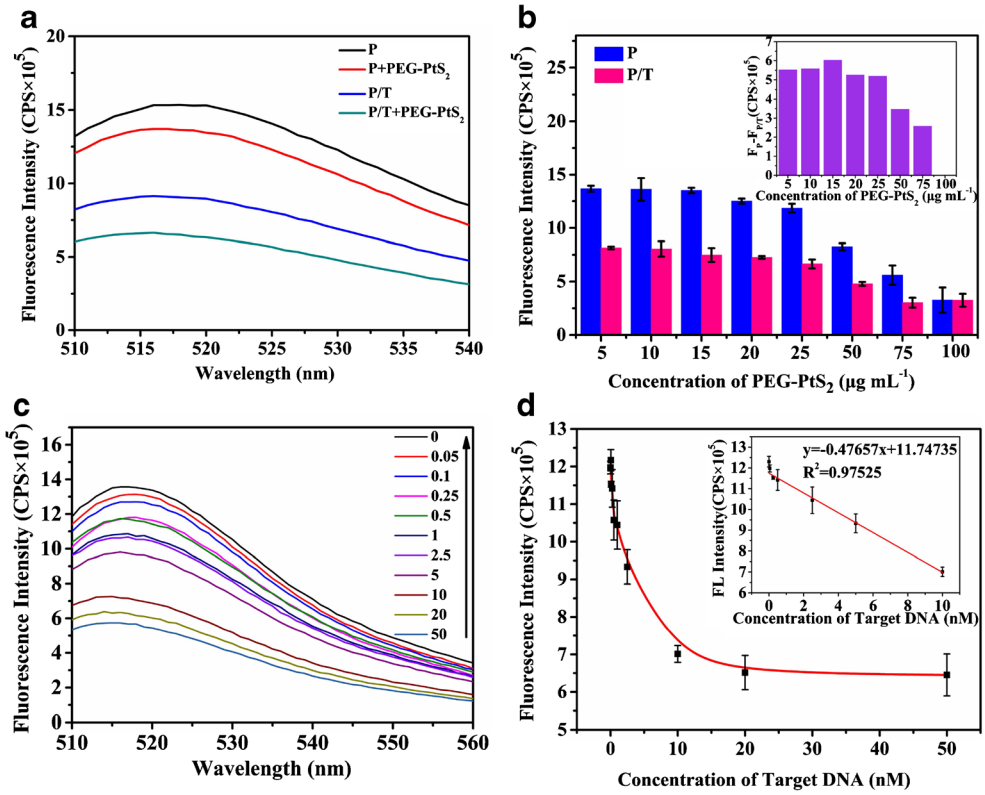

Fig. 2 PEG-PtS_2 nanosheet-based fluorescence biosensor for DNA determination. **a** Fluorescence spectra of P (10 nM) and P/T (10 nM) in the absence and presence of PEG-PtS_2 nanosheets (final concentration of 15.0 μg mL^{-1}). **b** Fluorescence intensity of P+PEG-PtS_2 (blue) and P/T+PEG-PtS_2 (red) in the presence of PEG-PtS_2 nanosheets at different final concentrations of 5, 10, 15, 20, 25, 50, 75, and 100 μg mL^{-1} (P: 10 nM, T: 10 nM). The error bars represented standard deviation of four parallel experiments. Inset: The fluorescence intensity *D*-value ($F_P - F_{P/T}$) at 517 nm in presence of PEG-PtS_2 nanosheets with different final concentrations of 5, 10, 15, 20, 25, 50, 75, and 100 μg mL^{-1} (P: 10 nM, T: 10 nM). **c** Fluorescence spectra of P in the presence of different concentrations of T (0, 0.05, 0.1, 0.25, 0.5, 1, 2.5, 5, 10, 20, 50 nM) with the addition of PEG-PtS_2 nanosheets (15 μg mL^{-1}). **d** Calibration plot of DNA determination. Inset: The linear plot of fluorescence peak intensity of P vs. the concentration of T with addition of PEG-PtS_2 nanosheets (15 μg mL^{-1}). The excitation and emission wavelengths were 468 and 517 nm, respectively. The error bars represented standard deviation of four parallel experiments

Table 1 The determination of HPV16 in human genomic DNA samples

Sample	Added (nM)	Detected (nM)	RSD (%) ($N = 4$)	Recovery (%)
1	2	1.96	1.33	98.0
2	4	4.01	3.32	96.4
3	6	6.11	3.43	102.7
4	8	8.10	2.13	101.3

without the need for probe immobilization and tedious washing steps.

Selectivity is an important parameter to evaluate the feasibility of a DNA biosensor. As shown in Fig. 3, by use of HPV16 as probe DNA, other HPV genotypes (HPV18, HPV33, and HPV58) with different sequences did not decrease the fluorescent intensity compared with the complementary HPV16 target sequence, which indicated that PEG-PtS_2 nanosheet-based fluorescent biosensor is selective for DNA genotyping.

To verify the practical application of the proposed method in clinical diagnosis, we determine HPV16 in clinical samples. The standard addition method was performed for the determination, in which the real sample was the human genomic DNA extracted from the clinical samples of cervical scraps. As shown in Table 1, the recovery rate of HPV16 genotype in human genomic DNA samples varied from 96.4 to 102.7%, and the relative standard deviation (RSD) was from 1.33 to 3.43%. The good precision revealed that this method has the potential for HPV16 determination in clinical DNA samples.

At present, for the determination of real samples, the target DNA fragment may still need to be amplified by PCR before determination, not to say single-molecule detection. It was necessary to select a more suitable fluorescent-labeled probe on this basis to enhance the signal difference and reduce the limit of detection.

We further investigated the fluorescence quenching mechanism of the dsDNA in the presence of PEG-PtS_2 nanosheets. As summarized from the literature, dynamic quenching effect (DQE) and static quenching effect (SQE) are two major reasons for fluorescence quenching. The fluorophore excited state and the quencher collide and the energy was released by nonradioactive deactivation in DQE process, while in SQE process, a nonfluorescent ground-state complex was formed between the fluorophore and the quencher. The energy absorbed by the generated complex was exhausted in the nonradioactive manner, and no photon emission was generated during the entire process [21–23]. Both DQE and SQE were theoretically consistent with the Stern-Volmer equation [23, 24]:

$$F_0/F = 1 + K_{SV}[Q]$$

where F_0 is the fluorescence intensity of only (ss/ds) DNA at 517 nm; F is the fluorescence intensity of the (ss/ds) DNA with

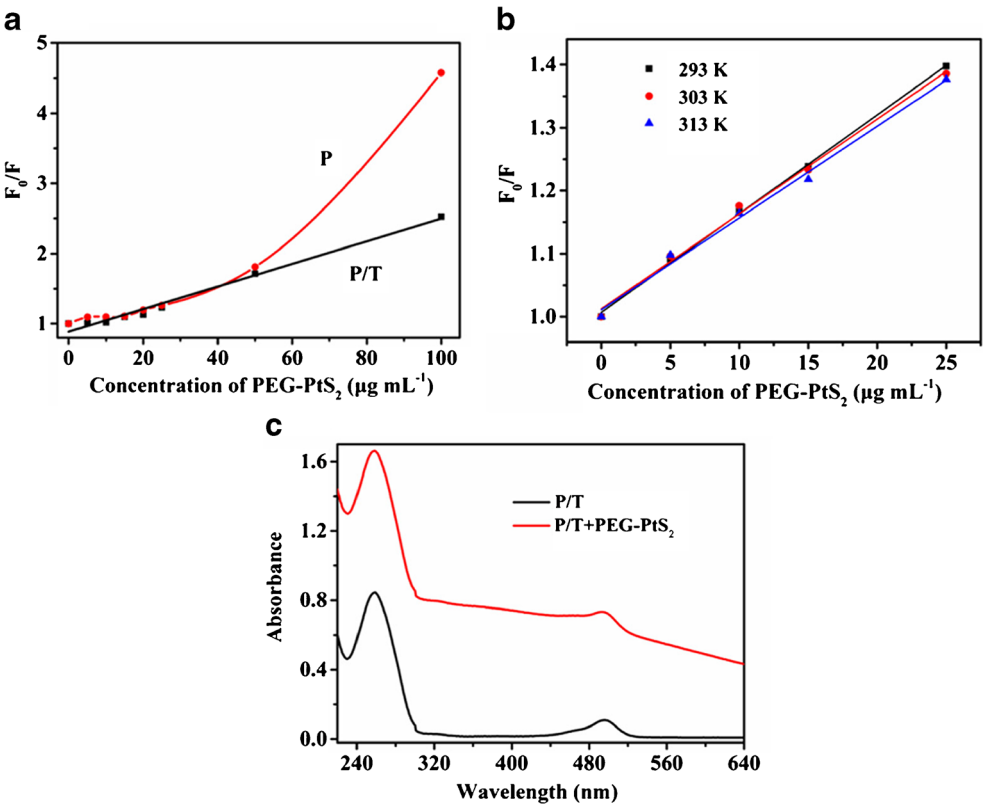

Fig. 4 **a** Stern-Volmer equation after the addition of PEG-PtS_2 nanosheets. **b** Stern-Volmer equation under different temperatures after the addition of PEG-PtS_2 nanosheets. **c** UV-vis absorption spectra of the dsDNA in the absence and presence of PEG-PtS_2 nanosheets

the addition of PEG-PtS_2 nanosheets; K_{SV} is the Stern-Volmer quenching constant; and [Q] is the concentration of PEG-PtS_2 nanosheets.

Generally, only one type of quenching mechanism exists in DQE or SQE when the Stern-Volmer plot is linear. The system involved both kinds of quenching mechanism when the Stern-Volmer plot reveals an upward or downward trend [25, 26]. As displayed in Fig. 4a (red curve), the Stern-Volmer plot performs an upward trend, indicating the existence of both DQE and SQE between ssDNA (P) and PEG-PtS_2. As shown in Fig. 4a (black curve), it could found a good linear relationship between dsDNA and the PEG-PtS_2 concentration, which revealed that either DQE or SQE existed during the quenching process. Nevertheless, it was difficult to distinguish DQE and SQE only by the Stern-Volmer equation. For the sake of clarifying the type of the quenching, we further measured fluorescence quenching constants under different temperatures of 293, 303, and 313 K. For the DQE, the constant value of fluorescence quenching increased with the increment of system temperature, while the value has a reversed trend as the fluorescence quenching constant will decrease with the rise of temperature in the SQE [27]. In the presence of PtS_2 nanosheets, the K_{SV} value displayed a decreasing trend with the increment of temperature (Fig. 4b). As obviously shown in Fig. 4c, a considerable change of the absorption spectrum of dsDNA(P/T) occurred by existence of the PEG-PtS_2, which indicates a ground-state complex formation and static quenching effect in the system. These results indicated that the mechanism of fluorescence quenching of PEG-PtS_2 nanosheet-based fluorescence biosensor for dsDNA might stem from static quenching effect.

Conclusion

We had successfully prepared PEG-PtS_2 nanosheets by an ultrasonication-assisted liquid exfoliation method and enhanced its dispersibility in the aqueous solution by pegylation. PEG-PtS_2 nanosheets possessed good fluorescence quenching capability, and thereafter, a novel fluorescent biosensor for HPV-16 genotyping was successfully developed. This one-step mix-and-detect assay format is simple and homogeneous, without the need of probe immobilization and tedious washing steps. The biosensor showed good sensitivity and selectivity, with the range between 0.05 and 10 nM and the LOD of 0.44 nM. This assay was also applicable for the clinical samples with good precision. The fluorescence quenching mechanism of PEG-PtS_2 nanosheet-based fluorescence biosensor for dsDNA might stem from static quenching effect. Further study will be focused on the selection of a more suitable fluorescent-labeled probe to enhance the signal difference and reduce the limit of detection. We believe this biosensor provides an opportunity to develop simple, fast, and low-cost strategy for molecular diagnostics.

Funding information This work was supported by grants from National Natural Science Foundation of China (21605160), Jiangsu Natural Science Foundation (BK20171387), "Double First-Class" University project (CPU2018GY25), Jiangsu Innovation and Enterpreneurship Project, and Open Research Fund of State Key Laboratory of Bioelectronics Southeast University, and Young Teachers' Research Funding from College of Science, China Pharmaceutical University.

Compliance with ethical standards

Conflict of interest The authors declare that they have no competing interests.

References

1. Piao J, Zhou X, Wu X (2018) Colorimetric human papillomavirus DNA assay based on the retardation of avidin-induced aggregation of gold nanoparticles. Microchim Acta 185(12):537
2. Yi C, Li C-W, Fu H, Zhang M, Qi S, Wong N-B, Lee S-T, Yang M (2010) Patterned growth of vertically aligned silicon nanowire arrays for label-free DNA detection using surface-enhanced Raman spectroscopy. Anal Bioanal Chem 397(7):3143–3150
3. Shi Q, Shi Y, Pan Y, Yue Z, Zhang H, Yi C (2015) Colorimetric and bare eye determination of urinary methylamphetamine based on the use of aptamers and the salt-induced aggregation of unmodified gold nanoparticles. Microchim Acta 182(3–4):505–511
4. Crosbie EJ, Einstein MH, Franceschi S, Kitchener HC (2013) Human papillomavirus and cervical cancer. Lancet 382(9895): 889–899
5. Yuan Y, Ma Y, Luo L, Wang Q, Huang J, Liu J, Yang X, Wang K (2019) Ratiometric determination of human papillomavirus-16 DNA by using fluorescent DNA-templated silver nanoclusters and hairpin-blocked DNAzyme-assisted cascade amplification. Microchim Acta 186(9):613
6. van Ham MA, Bakkers JM, Harbers GK, Quint WG, Massuger LF, Melchers WJ (2005) Comparison of two commercial assays for detection of human papillomavirus (HPV) in cervical scrape specimens: validation of the Roche AMPLICOR HPV test as a means to screen for HPV genotypes associated with a higher risk of cervical disorders. J Clin Microbiol 43(6):2662–2667
7. Li M-J, Wong KM-C, Yi C, Yam V-W (2012) New ruthenium(II) complexes functionalized with coumarin derivatives: synthesis, energy-transfer-based sensing of esterase, cytotoxicity, and imaging studies. Chem Eur J 18(28):8724–8730
8. Chhowalla M, Shin HS, Eda G, Li L-J, Loh KP, Zhang H (2013) The chemistry of two-dimensional layered transition metal dichalcogenide nanosheets. Nat Chem 5(4):263–275
9. Huang X, Zeng ZY, Zhang H (2013) Metal dichalcogenide nanosheets: preparation, properties and applications. Chem Soc Rev 42(5):1934–1946
10. Xu M, Liang T, Shi M, Chen H (2013) Graphene-like two-dimensional materials. Chem Rev 113(5):3766–3798
11. Tan C, Zhang H (2015) Two-dimensional transition metal dichalcogenide nanosheet-based composites. Chem Soc Rev 44(9):2713–2731
12. Li H, Wu J, Yin Z, Zhang H (2014) Preparation and applications of mechanically exfoliated single-layer and multilayer MoS2 and WSe2 nanosheets. Acc Chem Res 47(4):1067–1075

13. Xie J, Zhang J, Li S, Grote F, Zhang X, Zhang H, Wang R, Lei Y, Pan B, Xie Y (2013) Controllable disorder engineering in oxygen-incorporated MoS2 ultrathin nanosheets for efficient hydrogen evolution. J Am Chem Soc 136(4):17881–17888
14. Zhu C, Zeng Z, Li H, Li F, Fan C, Zhang H (2013) Single-layer MoS2-based nanoprobes for homogeneous detection of biomolecules. J Am Chem Soc 135(16):5998–6001
15. Late DJ, Huang YK, Liu B, Acharya J, Shirodkar SN, Luo J, Yan A, Charles D, Waghmare UV, Dravid VP (2013) Sensing behavior of atomically thin-layered MoS2 transistors. ACS Nano 7(6):4879–4891
16. Sun Y, Gao S, Xie Y (2014) Atomically-thick two-dimensional crystals: electronic structure regulation and energy device construction. Chem Soc Rev 43(2):530–546
17. Yuan J, Sun T, Hu Z, Yu W, Ma W, Zhang K, Sun B, Lau SP, Bao Q, Lin S (2018) Wafer-scale fabrication of two-dimensional PtS2/PtSe2 heterojunctions for efficient and broad band photodetection. ACS Appl Mater Interfaces 10(47):40614–40622
18. Wang X, Cheng PK, Tang CY, Long H, Yuan H, Zeng L, Ma S, Qarony W, Tsang YH (2018) Laser Q-switching with PtS2 microflakes saturable absorber. Opt Express 26(10):13055–13060
19. Long H, Tang CY, Cheng PK, Wang XY, Qarony W, Tsang YH (2018) Ultrafast laser pulses generation by using 2D layered PtS2 as a saturable absorber. J Lightwave Technol 37(4):1174–1179
20. Xu Z, Lou W, Wu X, Wang X, Hao J (2017) Investigating the tribological behavior of PEGylated MoS 2 nanocomposites as additives in polyalkylene glycol at elevated temperature. RSC Adv 7(84):53346–53354
21. Zhai W, Wang C, Yu P, Wang Y, Mao L (2014) Single-layer MnO2 nanosheets suppressed fluorescence of 7-hydroxycoumarin: mechanistic study and application for sensitive sensing of ascorbic acid in vivo. Anal Chem 86(24):12206–12213
22. Cui F-L, Yan Y-H, Zhang Q-Z, Qu G-R, Du J, Yao X-J (2010) A study on the interaction between 5-methyluridine and human serum albumin using fluorescence quenching method and molecular modeling. J Mol Model 16(2):255–262
23. Liu J, Chen Y, Wang L, Na M, Chen H, Chen X (2019) Modification-free fabricating ratiometric nanoprobe based on dual-emissive carbon dots for nitrite determination in food samples. J Agric Food Chem 67(13):3826–3836
24. Zhang Z, Pan Y, Fang Y, Zhang L, Chen J, Yi C (2015) Tuning photoluminescence and surface properties of carbon nanodots for chemical sensing. Nanoscale 8(1):500–507
25. Liu X, Zhang W, Yang C, Yao Y, Huang L, Li S, Wang J, Ji Y (2019) Rapid and selective fluorometric determination of tannic acid using MoO3-x quantum dots. Microchim Acta 186(4):247
26. Xu H, Yang X, Li G, Zhao C, Liao X (2015) Green synthesis of fluorescent carbon dots for selective detection of tartrazine in food samples. J Agric Food Chem 63(30):6707–6714
27. Sahoo D, Mandal A, Mitra T, Chakraborty K, Bardhan M, Dasgupta AK (2018) Nanosensing of pesticides by zinc oxide quantum dot: an optical and electrochemical approach for the detection of pesticides in water. J Agric Food Chem 66(2):414–423